

Superomniphobic surfaces: Design and durability

Arun K. Kota, Wonjae Choi, and Anish Tuteja

Surfaces that display liquid contact angles greater than 150° along with low contact angle hysteresis for liquids with both high and low surface tension values are known as superomniphobic surfaces. Such surfaces are of interest for a diverse array of applications, including self-cleaning surfaces, nonfouling surfaces, stain-free clothing, spill-resistant protective wear, drag reduction, and fingerprint-resistant surfaces. Recently, significant advances have been made in understanding the criteria required to design superomniphobic surfaces. In this article, we discuss the roles of surface energy, roughness, re-entrant texture, and hierarchical structure in fabricating superomniphobic surfaces. We also provide a review of different superomniphobic surfaces reported recently in the literature and emphasize the need for mechanical, chemical, and radiation durability of superomniphobic surfaces for practical applications. Finally, we conclude with a discussion of the unresolved challenges in developing durable superomniphobic surfaces that define the scope for further improvements in the field.

Introduction

Surfaces with extreme repellency to liquids have drawn significant interest for various civilian and military applications, including self-cleaning surfaces,[1] nonfouling surfaces,[2] stain-free clothing and spill-resistant protective wear,[3] drag reduction,[4] and locomotion of microrobots in aqueous and chemical environments.[5,6] Two commonly used measures of liquid repellency are the contact angle and contact angle hysteresis (i.e., the difference between the advancing [maximum] and receding [minimum] contact angles) on a solid surface (also see the Introductory article in this issue). A surface is considered super-repellent when it displays very high contact angles (typically >150° as shown in Figure 1a) *and* very low contact angle hysteresis (typically <5°) for a contacting liquid.[7] When a surface displays very high contact angles and high contact angle hysteresis, the liquid droplets stick to the surface (see **Figure 1**a–c). Unlike such "sticky nonwetting surfaces,"[8–14] super-repellent surfaces display low contact angle hysteresis and thereby facilitate easy roll off and bouncing of the contacting liquid droplets. Recently, a new type of super-repellent surface,[15–17] which displays low contact angles and low contact angle hysteresis, has also been reported (see Figure 1d). While liquid droplets can easily slide on such slippery surfaces, bouncing of liquid droplets[18] (see Figure 1e) is limited only to the conventional super-repellent surfaces.

Typically, super-repellent surfaces are considered to be superhydrophobic if they display contact angles >150° and contact angle hysteresis <5° with water, and superoleophobic if they display contact angles >150° and contact angle hysteresis <5° with low surface tension (typically γ_{LV} <30 mN/m) liquids such as oils and alcohols.[19–22] Most superoleophobic surfaces are also superhydrophobic because surfaces that can repel low surface tension liquids such as oils and alcohols can more easily repel water, which possesses a higher surface tension. However, recently, surfaces that are superoleophobic and yet superhydrophilic have been reported.[23,24] In view of such counterintuitive surfaces, we define surfaces that display *both* superhydrophobicity and superoleophobicity as superomniphobic surfaces.[25]

One of the first reports on surfaces displaying very high contact angles with oils dates back to the work of Tsujii et al.[26] in 1997. Recently, significant advances have been made in understanding the criteria required to design superomniphobic surfaces. In this article, we discuss the systematic design of superomniphobic surfaces with specific emphasis on the role of surface roughness and re-entrant texture (i.e., convex topography). We also discuss how surfaces with hierarchical scales of texture (i.e., more than one length scale of texture) display higher contact angles and lower contact angle hysteresis with a contacting liquid by entrapping air at multiple length scales,

Arun K. Kota, Department of Materials Science and Engineering, University of Michigan; arunkota@umich.edu
Wonjae Choi, Department of Mechanical Engineering, University of Texas at Dallas; wonjae.choi@utdallas.edu
Anish Tuteja, Department of Materials Science and Engineering, University of Michigan; atuteja@umich.edu
DOI: 10.1557/mrs.2013.101

© 2013 Materials Research Society

https://doi.org/10.1557/mrs.2013.101 Published online by Cambridge University Press

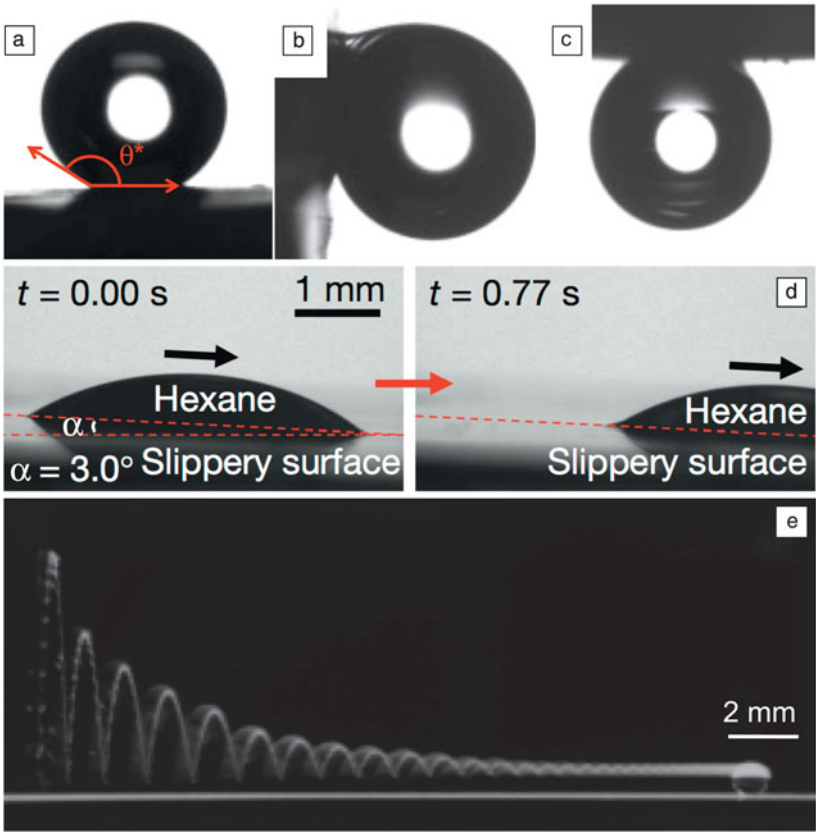


Figure 1. (a–c) A "sticky nonwetting surface" with a droplet of water displaying a very high contact angle (θ* >150°) and sticking to the surface tilted by 0°, 90°, and 180°, respectively, relative to the horizontal. Reprinted with permission from Reference 11. © 2005 Wiley. (d) A slippery super-repellent surface with a droplet of hexane displaying a low contact angle but sliding off when the surface is tilted by α = 3° relative to horizontal, indicating low contact angle hysteresis. Reprinted with permission from Reference 17. © 2011 Nature Publishing Group. (e) An impinging droplet of water bounces several times and rolls off of a conventional super-repellent surface tilted by 1° relative to the horizontal. Reprinted with permission from Reference 18. © 2000 IOP Publishing. Note: *t*, time.

thereby reducing the solid-liquid contact area. Further, we provide a review of how researchers have engineered different superomniphobic surfaces in the past few years. Practical applications of superomniphobic surfaces in stain-free clothing, spill-resistant protective wear, drag reduction, and chemical shielding require good mechanical, chemical, and radiation durability. For example, laundering a superomniphobic fabric subjects it to a combination of highly aggressive processes containing chemicals and mechanical stresses. With this in view, we give examples of the current state-of-the-art durable superomniphobic surfaces and present the unresolved challenges that define the scope for further improvements in the field.

Designing superomniphobic surfaces

Superomniphobic surfaces display high contact angles and low contact angle hysteresis for virtually all liquids, including low surface tension liquids. In this section, we will first discuss the importance of roughness and re-entrant texture of a surface in obtaining high contact angles and low contact angle hysteresis with low surface tension liquids. Subsequently, we will discuss the importance of hierarchically structured surfaces in further increasing the contact angles and decreasing the contact angle hysteresis.

The primary measure of wetting of a liquid on a non-textured (or smooth) surface is the equilibrium contact angle θ, given by Young's relation[27] as (see the Introductory article in this issue):

$$\cos\theta = \frac{\gamma_{SV} - \gamma_{SL}}{\gamma_{LV}}. \quad (1)$$

Here, γ refers to the interfacial tension, and the subscripts S, L, and V refer to the solid, liquid, and vapor phases, respectively. When a droplet of liquid contacts a textured substrate, it can adopt one of the following two configurations to minimize its overall free energy[28–32]—the Wenzel[33] state or the Cassie–Baxter[34] state. In the Wenzel state, as shown in **Figure 2**a, the contacting liquid droplet completely permeates the surface protrusions, forming the so-called "fully-wetted" interface. In this state, the apparent contact angle θ* (i.e., the contact angle on a textured surface) is calculated using the Wenzel relation:[33]

$$\cos\theta^* = r\cos\theta. \quad (2)$$

Here, *r* is the surface roughness, defined as the ratio of the actual surface area to the projected surface area. Since *r* is always greater than unity, roughness amplifies both the wetting and nonwetting behavior of materials in the Wenzel state. In other words, $\cos\theta^* >> 0$ if $\cos\theta > 0$ and $\cos\theta^* << 0$ if $\cos\theta < 0$. It should be noted that a droplet may not display the apparent contact angle described by Equation 2 due to contact line pinning at numerous surface asperities, which in turn increases the contact angle hysteresis.[35,36]

On the other hand, in the Cassie–Baxter state, as shown in Figure 2b, the liquid does not completely wet the surface texture. Instead, pockets of air remain trapped underneath the liquid droplet. The liquid penetrates into the surface texture until the local texture angle (ψ) becomes equal to the equilibrium contact angle θ (given by Young's relation) for the three-phase contact line.[30,31,37] Consequently, substrates possessing re-entrant surface texture (i.e., texture angle $\psi < 90°$) can support a composite (solid-liquid-air) interface even for low surface tension liquids, such as oils and alcohols, which display Young's contact angles $\theta < 90°$ (see Figure 2b). The apparent contact angles in this state are typically calculated using the Cassie–Baxter relation,[34] given as:

$$\cos\theta^* = f_{SL}\cos\theta + f_{LV}\cos\pi = f_{SL}\cos\theta - f_{LV}. \quad (3)$$

https://doi.org/10.1557/mrs.2013.101 Published online by Cambridge University Press

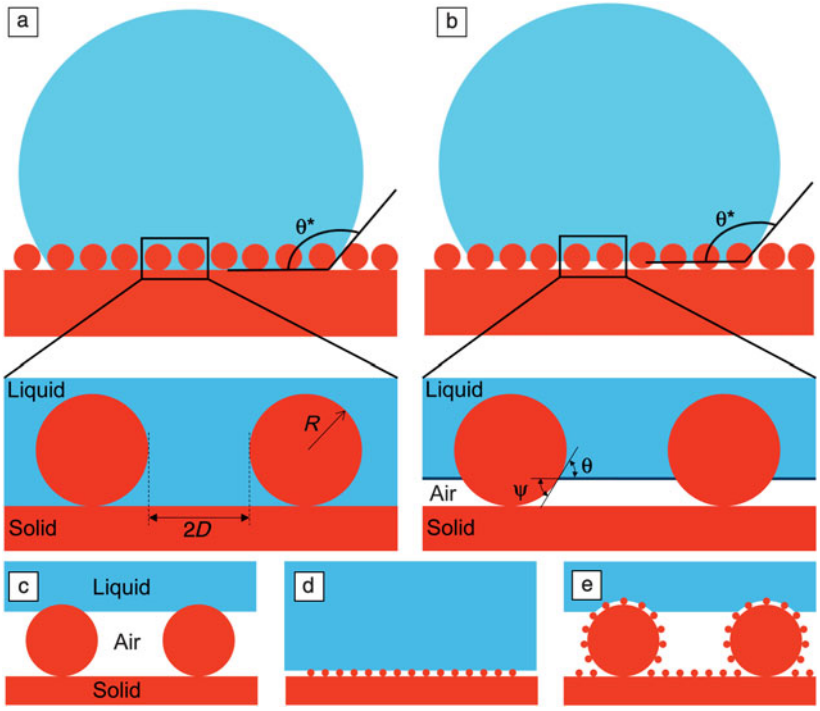


Figure 2. (a–b) Schematic of a liquid droplet in the Wenzel state and the Cassie–Baxter state, respectively, on a textured solid surface. (c–e) Schematics for a liquid droplet in the Cassie–Baxter state on a coarser textured surface, a finer textured surface, and a hierarchically textured surface, respectively. Note: θ*, apparent contact angle; θ, contact angle; ψ, local texture angle; *R*, radius of the feature; *D*, half the inter-feature spacing.

Here, f_{SL} is the area fraction of the solid-liquid interface, and f_{LV} is the area fraction of the liquid-air interface underneath the liquid droplet on a homogeneous surface. Note that for nonhomogeneous surfaces, f_{SL} and f_{LV} represent the local areal fractions of the solid-liquid interface and the liquid-air interface, respectively, in the vicinity of the three phase (solid-liquid-vapor) contact line.[36] In contrast to the Wenzel state, high values of f_{LV} in the Cassie–Baxter state promote high apparent contact angles and low contact angle hysteresis even for low surface tension liquids.[35,38,39] Consequently, substrates with re-entrant surface texture that can lead to the formation of the Cassie–Baxter state even with low surface tension liquids are critical for designing superomniphobic surfaces.

Hierarchically structured surfaces, such as the lotus leaf,[1,18] possess more than one scale of texture (a finer length scale texture on an underlying coarser length scale texture; see Figure 2c–e). When a hierarchically structured surface supports a contacting liquid droplet in the Cassie–Baxter state at all length scales, the liquid droplet displays higher apparent contact angles compared to surfaces that possess a single scale of texture. This is because of the air trapped at both the coarser length scale, as well as the finer length scale (see Figure 2e). The apparent contact angles on a hierarchical surface can be calculated by recursively writing the Cassie–Baxter relation as[40,41]

$$\cos\theta^*_n = \left(1 - f_{LV,n}\right)\cos\theta^*_{n-1} - f_{LV,n}. \quad (4)$$

Here, n = 1, 2, 3 and so on and is the number of length scales of texture, $f_{LV,n}$ is the area fraction of the liquid-air interface for the n^{th} scale of texture, and θ^*_n and θ^*_{n-1} are the apparent contact angles on hierarchically structured surfaces with n scales of texture and n–1 scales of texture, respectively. From Equation 4, it is evident that θ^*_n increases as the number of scales of texture n increases.

Hierarchically textured surfaces that support a contacting droplet in the Cassie-Baxter state also display a lower contact angle hysteresis compared to surfaces that possess a single scale of texture.[7,42–46] Contact angle hysteresis is related to energy barriers that a liquid droplet must overcome during its movement along a solid surface, and thus characterizes the resistance to the droplet movement.[28,47] Lower solid-liquid contact area leads to less contact line pinning (i.e., lower resistance to droplet movement) and consequently lower contact angle hysteresis. Typically, hierarchically structured surfaces have a significantly lower solid-liquid contact area compared to surfaces that possess a single scale of texture (see Figure 2e). This can lead to significantly lower contact angle hysteresis.[7,42–46]

In addition, theoretical analysis[31] has shown that surfaces with two scales of texture can enhance the stability of the Cassie–Baxter state by providing more locations with re-entrant texture where the composite interface can be stable. Recent work[48,49] has also shown that the overall free energy increasingly favors the Cassie–Baxter state over the Wenzel state with an increasing number of scales of texture. For all these reasons, hierarchically structured surfaces possessing re-entrant texture are ideal for developing superomniphobic surfaces.

Recent work on superomniphobic surfaces

Several researchers have engineered superomniphobic surfaces utilizing hierarchically structured surfaces with re-entrant texture. However, there are two important criteria that are sometimes neglected in the literature on this subject. First, superomniphobic surfaces should display contact angles greater than 150° with low surface tension liquids *and* low contact angle hysteresis (Δθ*). Just reporting an apparent contact angle (θ*) or an apparent advancing (i.e., maximum) contact angle (θ^*_A) greater than 150° for an oil or an alcohol does not adequately describe superomniphobicity. The apparent receding (i.e., minimum) contact angle (θ^*_R), contact angle hysteresis, or roll-off angle (i.e., the minimum angle α by which the surface must be tilted relative to the horizontal for the droplet to roll-off) must also be diligently measured and reported because they are useful in estimating the ease of droplet roll-off and bouncing. Obtaining low contact angle hysteresis (typically

https://doi.org/10.1557/mrs.2013.101 Published online by Cambridge University Press

$\Delta\theta^* < 5°$) and low roll-off angles (typically $\alpha < 5°$) for oils or alcohols is perhaps as important as the maximum achievable contact angle in qualifying a surface as superomniphobic. Second, there is sometimes a lack of clarity regarding which liquid or liquids must be used in qualifying a surface as superomniphobic. In the literature, it is sometimes difficult to compare across different superomniphobic surfaces because many liquids ranging in surface tension from heptane (γ_{LV} = 20.1 mN/m) to diiodomethane (γ_{LV} = 50.8 mN/m) have been used for wettability measurements. Sometimes, the surface tension of the oil or alcohol is not mentioned at all. In order to allow easier comparison with other reports in the literature, it is important to measure and report the contact angle hysteresis $\Delta\theta^*$ or roll-off angles α for a variety of liquids possessing a low surface tension.

Cao et al.[50] fabricated hierarchically structured porous silicon films by a gold-assisted electroless etching process. Upon silanization with perfluorooctyl trichlorosilane, the surfaces displayed an apparent contact angle θ^* = 151° with hexadecane (γ_{LV} = 27.5 mN/m). Leng et al.[3] fabricated hierarchically textured cotton textiles that were coated first with positively charged silica microparticles and then with negatively charged silica nanoparticles (see **Figure 3**a–b). First, the silica microparticles were covalently attached to the cotton textile via an *in situ* Stober reaction (i.e., tetraethyl orthosilicate was added to an aqueous solution of ammonia, methanol, and propanol). Upon treating this surface with 3-aminopropyl triethoxysilane (APS) and protonation with hydrochloric acid, the surface charge turned positive. Negatively charged silica nanoparticles were then electrostatically adsorbed onto the surface by dip-coating. Upon silanization of this hierarchically textured surface with perfluorodecyl trichlorosilane, the surfaces displayed an apparent contact angle as high as θ^* = 152° and a roll-off angle as low as α = 9° with hexadecane. Hsieh et al.[51] fabricated silica sphere stacks with two-tier hierarchical texture by using a two-stage spin coating technique. When the surfaces were further spin-coated with a perfluoroalkyl methacrylic copolymer to reduce the solid surface energy, they displayed an advancing contact angle $\theta_A^* \approx 150°$ and contact angle hysteresis $\Delta\theta^* \approx 3°$ for hexadecane. They also measured the contact angle hysteresis for a wide variety of liquids with γ_{LV} = 23.4 mN/m to γ_{LV} = 72.1 mN/m and demonstrated that the contact angle hysteresis increased with decreasing γ_{LV} on their surfaces. Wang et al.[52] fabricated a hierarchical texture consisting of well-aligned titanium dioxide nanotubes on micropillars of titanium by laser micromachining and anodization. Upon silanization with perfluorooctyl trichlorosilane, the surfaces were superomniphobic with apparent contact angles θ^* = 155°, 156°, and 157° and roll-off angles α = 7°, 6°, and 5° for hexadecane, colza oil, and crude oil, respectively.

Fujii et al.[53] fabricated a dual scale pillared structure of aluminum-niobium (Al-Nb) alloy by combining oblique angle magnetron sputtering deposition (OAD) with anodic oxidation (see Figure 3c–e). First, discrete pillars of Al-Nb alloy were deposited on a scalloped aluminum substrate via OAD. Then, the deposited pillars were anodized in hot phosphate-glycerol electrolyte to form a nanoporous oxide layer. Upon modification of this hierarchically textured surface with fluoroalkyl phosphate (FAP), the surfaces displayed superomniphobicity with θ^* = 156° and 151° and $\Delta\theta^*$ = 2° and 6° for rapeseed oil (γ_{LV} = 35.7 mN/m) and hexadecane, respectively. Daramanin et al.[54] fabricated hierarchical structures by electrochemically depositing nanoporous films of poly(3,4- ethylenedioxypyrrole) on SU-8 (photoresist) micropillar surfaces. These substrates displayed advancing contact angles θ_A^* = 153° and 155°, and contact angle hysteresis $\Delta\theta^*$ = 35° and 4° for hexadecane

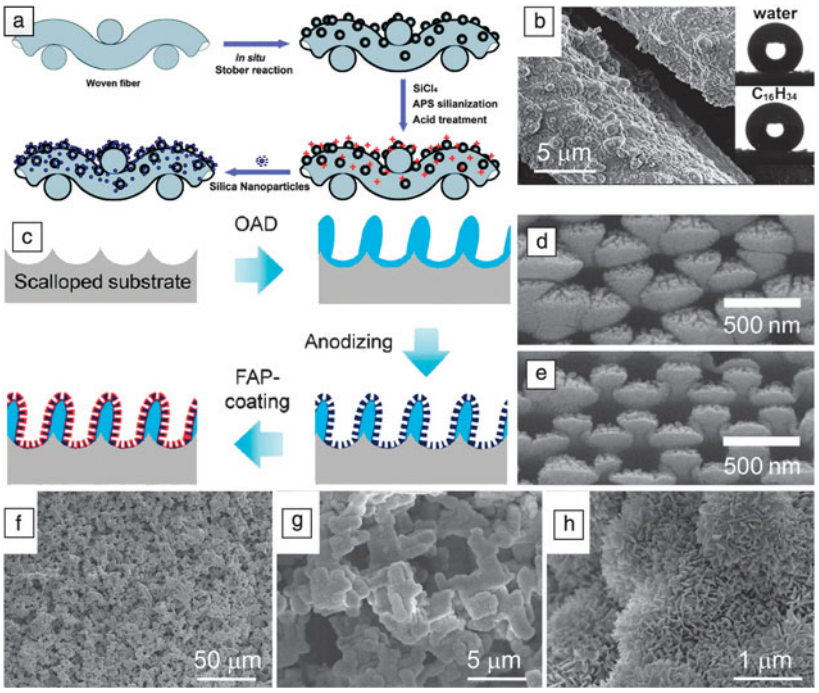


Figure 3. (a) Schematic illustrating the fabrication of hierarchically textured superomniphobic cotton textiles coated with silica micro- and nanoparticles. (b) A scanning electron microscopy (SEM) image of the resulting hierarchically textured cotton textile. Insets show droplets of water and hexadecane ($C_{16}H_{34}$) displaying high contact angles on the surface. Reprinted with permission from Reference 3. © 2009 American Chemical Society. (c) Schematic illustrating the fabrication of a dual scale pillared superomniphobic structure of an aluminum-niobium alloy. (d–e) SEM images of the resulting surface with different inter-feature spacing. Reprinted with permission from Reference 53. © 2011 American Chemical Society. (f) An SEM image of the hierarchically textured superomniphobic aluminum surface. (g–h) Magnified SEM images showing the coarser texture and the finer texture, respectively. Reprinted with permission from Reference 55. © 2011 Royal Society of Chemistry. Note: APS, 3-aminopropyl triethoxysilane; OAD, oblique angle magnetron sputtering deposition; FAP, fluoroalkyl phosphate.

https://doi.org/10.1557/mrs.2013.101 Published online by Cambridge University Press

and sunflower oil (γ_{LV} = 31 mN/m), respectively. Yang et al.[55] fabricated hierarchically structured surfaces of aluminum by etching aluminum in hydrochloric acid and subsequently dipping the etched structure in boiling water (see Figure 3f–h). Upon modifying the surface with perfluorooctanoic acid, it displayed apparent contact angles θ* = 158°, 156°, 155°, and 152°, contact angle hysteresis Δθ* = 5°, 8°, 18°, and 45°, and roll-off angles α = 5°, 7°, 15°, and 40°, for rapeseed oil, hexadecane, dodecane (γ_{LV} = 25.3 mN/m), and decane (γ_{LV} = 23.8 mN/m), respectively.

In our recent work,[45] we fabricated hierarchically structured superomniphobic surfaces with a PMMA (poly (methylmethacrylate))/fluorodecyl POSS (perfluorodecyl polyhedral oligomeric silsesquioxane) coating (see **Figure 4**a–c) that displayed high contact angles (θ^*_A = 155°; see Figure 4d) and ultralow contact angle hysteresis (Δθ* ≤ 4°) even with extremely low surface tension liquids such as heptane (γ_{LV} = 20.1 mN/m). Previous work[19,20,41] has demonstrated the synthesis of fluorodecyl POSS molecules, which possess one of the lowest known surface energies (γ_{SV} ≈ 10 mN/m). The addition of fluorodecyl POSS molecules to different polymers leads to a rapid decrease in the overall surface energy of the synthesized blends. The hierarchically structured surfaces developed in our work were fabricated by electrospinning microbeads (finer length scale texture with radius R ≈ 3–5 μm) of 50 wt% fluorodecyl POSS + PMMA blend (γ_{SV} = 10.3 mN/m) onto stainless steel wire meshes (coarser length scale texture with radius R ≈ 50–100 μm). Note that both the finer and coarser length scales possess re-entrant texture. The ultralow contact angle hysteresis of the superomniphobic surfaces allowed droplets of heptane (roll-off angles α ≤ 2°) and liquids of higher surface tension than heptane to easily roll-off and bounce[45] (see Figure 4e).

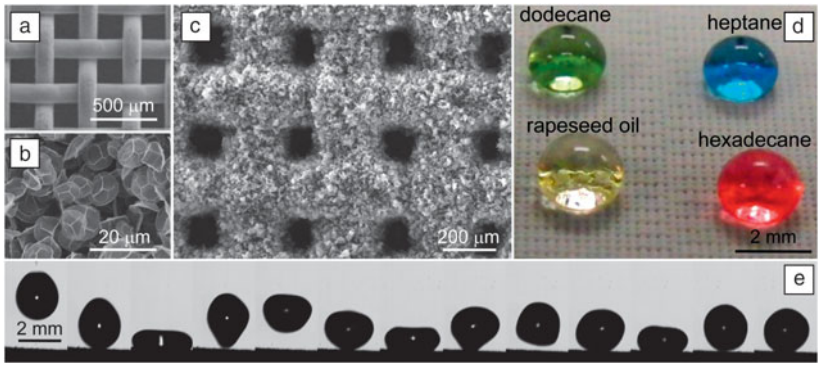


Figure 4. (a) Scanning electron microscopy (SEM) image of the coarser texture, which consists of a stainless steel wire mesh dip-coated with polymethylmethacrylate (PMMA) + perfluorodecyl polyhedral oligomeric silsesquioxane (fluorodecyl POSS) blend. (b) SEM image of the finer texture, which consists of electrospun beads of PMMA + fluorodecyl POSS blend. (c) SEM image of the hierarchically textured superomniphobic surface, which consists of electrospun beads of PMMA + fluorodecyl POSS blend on a stainless steel wire mesh. (d) Droplets of various low surface tension liquids displaying very high contact angles on the hierarchically textured surface. (e) A series of snapshots from a high-speed camera showing a droplet of heptane bouncing and rolling off of the hierarchically textured surface. Reprinted with permission from Reference 45. © 2012 Wiley.

In this manner, with an understanding of the importance of hierarchical structure and re-entrant texture, several researchers have engineered superomniphobic surfaces. A wide variety of materials ranging from metals to polymers and a wide variety of surface coatings ranging from perfluoralkyl silanes to perfluoroalkyl polyhedral oligomeric silsesquioxanes have been used for the fabrication of superomniphobic surfaces. These results pave the way for further research on developing durable superomniphobic surfaces that are necessary for many practical applications, as described later.

Durable superomniphobic surfaces

Practical applications of superomniphobic surfaces require good mechanical, chemical, and radiation durability. However, developing durable superomniphobic surfaces has thus far been a challenge. Under large external shear forces, the mechanical durability of a hierarchically structured superomniphobic surface may be compromised because most fine scale textures (typically on the nanoscale) are very delicate and can get damaged easily. Further, the finer scale texture, which usually possesses a low surface energy, can easily delaminate because it inherently exhibits low adhesion to the underlying surface. This problem becomes even more pronounced when the finer scale texture is not chemically bonded to the underlying coarser texture. These issues are somewhat similar to the challenges faced by hierarchically structured superhydrophobic surfaces.

The industrial perspective on the challenges associated with superhydrophobic surfaces is perhaps best provided by Extrand:[56] "during one of our technology update forums, we showed water bouncing off a super-hydrophobic surface. …The initial response was a combination of amazement and excitement. Enthusiasm quickly waned when one of our executives innocently touched the surface with his finger, destroying its superhydrophobic nature." The problem faced by superomniphobic surfaces is perhaps even more pronounced because of the additional requirement for re-entrant texture. One way of potentially improving the mechanical durability is to utilize monolithic hierarchical structures of mechanically robust materials instead of top-down approaches for depositing the finer scale texture. However, such surfaces are yet to be realized. Similarly, chemical and radiation durability calls for the careful choice of materials that are resistant to harsh chemical environments (such as concentrated acids, bases, and solvents) and radiation environments (ultraviolet [UV], infrared, and ozone), respectively. While there is significant scope for developing superomniphobic surfaces with high mechanical, chemical, and radiation durability, there are few reports that address these issues. We provide here a review of some of the reports on durable, hierarchically structured, superomniphobic surfaces.

https://doi.org/10.1557/mrs.2013.101 Published online by Cambridge University Press

Zhang et al.[57] fabricated glass slides coated with nanofilaments of trichloromethylsilane (TCMS) by regulating the water concentration during hydrolysis and condensation of TCMS (see **Figure 5**a). Upon converting the methyl groups on the surface of the nanofilaments into hydroxy groups with oxygen plasma and subsequent silanization with perfluorodecyl trichlorosilane (PFDTS), the surfaces turned transparent and superomniphobic for a wide variety of liquids, including mineral oil (γ_{LV} = 32 mN/m, θ* = 172°, α = 1.2°), toluene (γ_{LV} = 28.4 mN/m, θ* = 168°, α = 2.5°), *p*-xylene (γ_{LV} = 28.3 mN/m, θ* = 171°, α = 3.0°), hexadecane (θ* = 174°, α = 2.0°), dodecane (θ* = 167°, α = 2.3°), cyclohexane (γ_{LV} = 25 mN/m, θ* = 157°, α = 5.7°), and decane (θ* = 163°, α = 5.3°). These surfaces were reported to be stable against outdoor conditions, ozone, deep UV, sodium hydroxide, sulfuric acid, organic solvents (see Figure 5b), and temperatures up to 200°C for 24 hours. While the chemical and radiation durability of the surface is good, they reported that the mechanical durability needs significant improvement.

Wang et al.[58] fabricated superomniphobic surfaces by dip-coating plain weave polyester fabrics in a solution of fluorodecyl POSS + fluoroalkyl silane in ethanol (see Figure 5c).

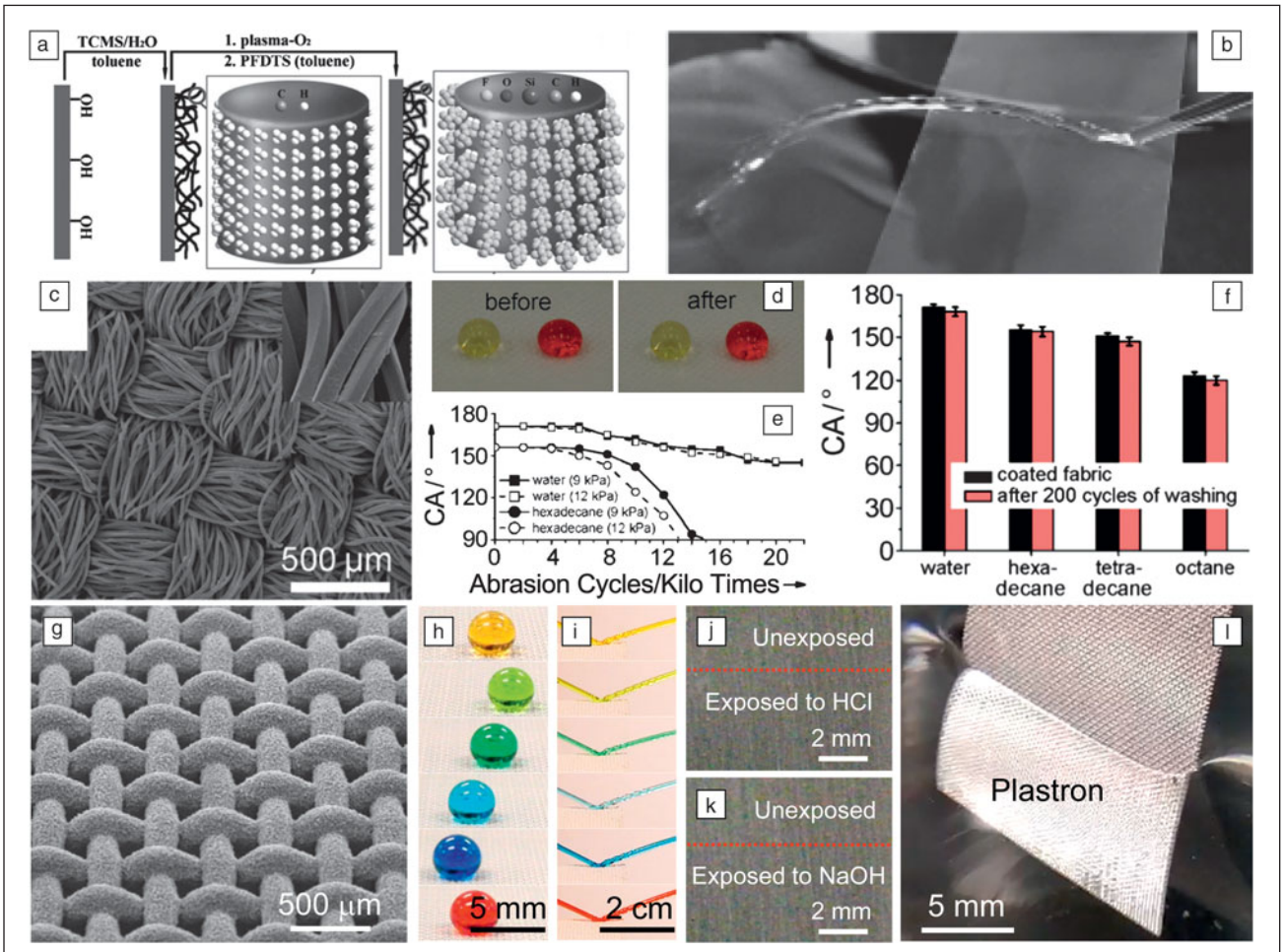


Figure 5. (a) A schematic depicting the fabrication of superomniphobic surfaces with fluorinated nanofilaments of silanes. (b) A jet of toluene bouncing off of the superomniphobic surface, indicating its chemical durability. Reprinted with permission from Reference 57. © 2011 Wiley. (c) A scanning electron microscopy (SEM) image of a superomniphobic polyester fabric fabricated by dip-coating in a solution of fluorodecyl POSS (perfluorodecyl polyhedral oligomeric silsesquioxane) + fluoroalkyl silane in ethanol. (d) Droplets of water (yellow) and hexadecane (red) do not show change in contact angles upon exposing the superomniphobic fabric to concentrated sulfuric acid. (e) Contact angles (CAs) of the water and hexadecane droplets on the superomniphobic fabric as a function of the number of abrasion cycles. (f) Contact angles of various liquids before and after the superomniphobic fabric is subjected to 200 cycles of standard machine laundry. The fabrics withstand 6000 cycles of abrasion at 9 kPa and 200 cycles of standard machine laundry without decrease in contact angles, indicating good mechanical durability. Reprinted with permission from Reference 58. © 2011 Wiley. (g) SEM image of the hierarchically textured superomniphobic surface, which consists of a stainless steel wire mesh electrospun with cross-linked PDMS (poly(dimethylsiloxane)) + fluorodecyl POSS blend. (h–i) Various Newtonian liquids (from top to bottom: yellow—dimethyl formamide, light green—toluene, dark green—acetic acid, light blue—hexadecane, dark blue—hexylamine, red—PDMS) display high contact angles and easily bounce on the hierarchically textured superomniphobic surface. (j–l) The electrospun coatings remain unaffected even upon extended exposure to concentrated hydrochloric acid, concentrated sodium hydroxide, and PDMS, respectively. The stable plastron layer in (l) indicates that surface does not reconfigure even when exposed to an enthalpically favorable solvent. Reprinted with permission from Reference 46. © 2012 American Chemical Society. Note: TCMS, trichloromethylsilane; PFDTS, perfluorodecyl trichlorosilane.

https://doi.org/10.1557/mrs.2013.101 Published online by Cambridge University Press

The dip-coated fabrics were superomniphobic for a wide variety of liquids, including toluene ($\theta^* = 159°$) and hexadecane ($\theta^* = 156°$, $\alpha = 4°$). The surfaces were reported to be stable against UV and concentrated sulfuric acid for 24 hours (see Figure 5d). Most significantly, the fabrics were reported to withstand 6000 cycles of abrasion at 9 kPa (see Figure 5e) and 200 cycles of standard machine laundry (see Figure 5f) without any change in the contact angles. The good mechanical durability is possibly due to a covalently bonded fluoroalkyl silane network that is embedded with fluorodecyl POSS molecules. However, the surfaces showed severe damage when exposed to potassium hydroxide.

In our recent work,[46] we fabricated hierarchically structured superomniphobic surfaces, which possess re-entrant texture at both the finer and coarser length scales, by electrospinning 50 wt% fluorodecyl POSS + cross-linked poly(dimethylsiloxane) (PDMS) blend (γ_{SV} = 11.5 mN/m) on top of stainless steel wire meshes (see Figure 5g). Virtually all Newtonian liquids (i.e., liquids for which viscosity is independent of the applied shear rate), including concentrated organic and inorganic acids, bases, and solvents, displayed very high apparent contact angles ($\theta^* > 150°$, see Figure 5h) and could easily roll off ($\alpha \leq 2°$) and bounce (see Figure 5i) on the hierarchically structured superomniphobic surfaces. The electrospun coatings remained unaffected (i.e., without any additional macroscopic or microscopic rough features due to corrosion or dissolution) even upon extended exposure to a wide range of concentrated acids (see Figure 5j), concentrated bases (see Figure 5k), organic solvents, or even PDMS itself (see Figure 5l). The stable plastron (i.e., air pockets) layer, formed when the hierarchically structured superomniphobic surface is submerged in uncross-linked oligomeric PDMS (see Figure 5l), indicates that the surface does not reconfigure even when exposed to an enthalpically favorable solvent. Another unique and remarkable feature of these surfaces is that they displayed superomniphobicity with a wide range of non-Newtonian liquids,[59,60] including polymer solutions of different polymer molecular weights, concentrations, and solvents. Due to such effective repellency and chemical durability, these surfaces can act as chemical shields against a range of different non-Newtonian liquids, in addition to Newtonian liquids.

Deng et al.[61] developed a technique to coat a porous layer of candle soot with silica via chemical vapor deposition of tetraethoxysilane catalyzed by ammonia. Upon calcination and silanization with perfluorooctyl trichlorosilane, the surfaces were transparent and superomniphobic for a wide variety of liquids, including peanut oil (γ_{LV} = 34.5 mN/m, $\theta^* = 158°$, $\alpha = 4°$), olive oil (γ_{LV} = 32 mN/m, $\theta^* = 157°$, $\alpha = 4°$), hexadecane ($\theta^* = 156°$, $\alpha = 5°$), and tetradecane ($\gamma_{LV} = 26.5$ mN/m, $\theta^* = 154°$, $\alpha = 5°$). The surfaces were reported to be reasonably stable under continuous drop impact, sand abrasion, and annealing up to 400°C, but they showed damage under peel tests.

One potential methodology to improve the mechanical durability is by developing self-healing superomniphobic surfaces. Although such surfaces cannot prevent damage, they possess an inherent healing mechanism that restores the superomniphobicity. Recently, Wang et al.[62] fabricated superomniphobic surfaces utilizing hierarchically structured porous aluminum surfaces that were fluorinated using perfluorooctanoic acid. Inspired by the recovery of superhydrophobicity of a lotus leaf after damage by the release of wax, they developed self-healing superomniphobic surfaces. In order to accomplish this, the pores in the fluorinated aluminum structure were pre-filled with perfluorooctanoic acid. Upon mildly damaging the surface with O_2 plasma, the surface automatically healed itself in 48 h at room temperature by the reaction of perfluorooctyl acid loaded in pores with the plasma-treated surface. However, the treatment is limited only to mild damage in surface chemistry and cannot address mechanical damage. In short, fabricating durable superomniphobic surfaces remains an active and exciting area of research.

Summary

We have discussed how superomniphobic surfaces can be designed using hierarchically structured surfaces possessing re-entrant texture. Recent studies have demonstrated the fabrication of superomniphobic surfaces using a wide variety of materials, fabrication methodologies, and fluorination techniques. We have emphasized that it is important to diligently characterize both contact angles and contact angle hysteresis for a variety of low surface tension liquids to qualify a surface as superomniphobic. We have also presented the current state-of-the-art durable superomniphobic surfaces and discussed the challenges and some potential strategies to improve mechanical, chemical, and radiation durability.

Acknowledgments

We thank Charles Y.-C. Lee and the Air Force Office of Scientific Research (AFOSR) for financial support under grants FA9550–11–1-0017. We also thank the donors of the Office of Naval Research (ONR) for financial support under Grant N00014-12-1-0874.

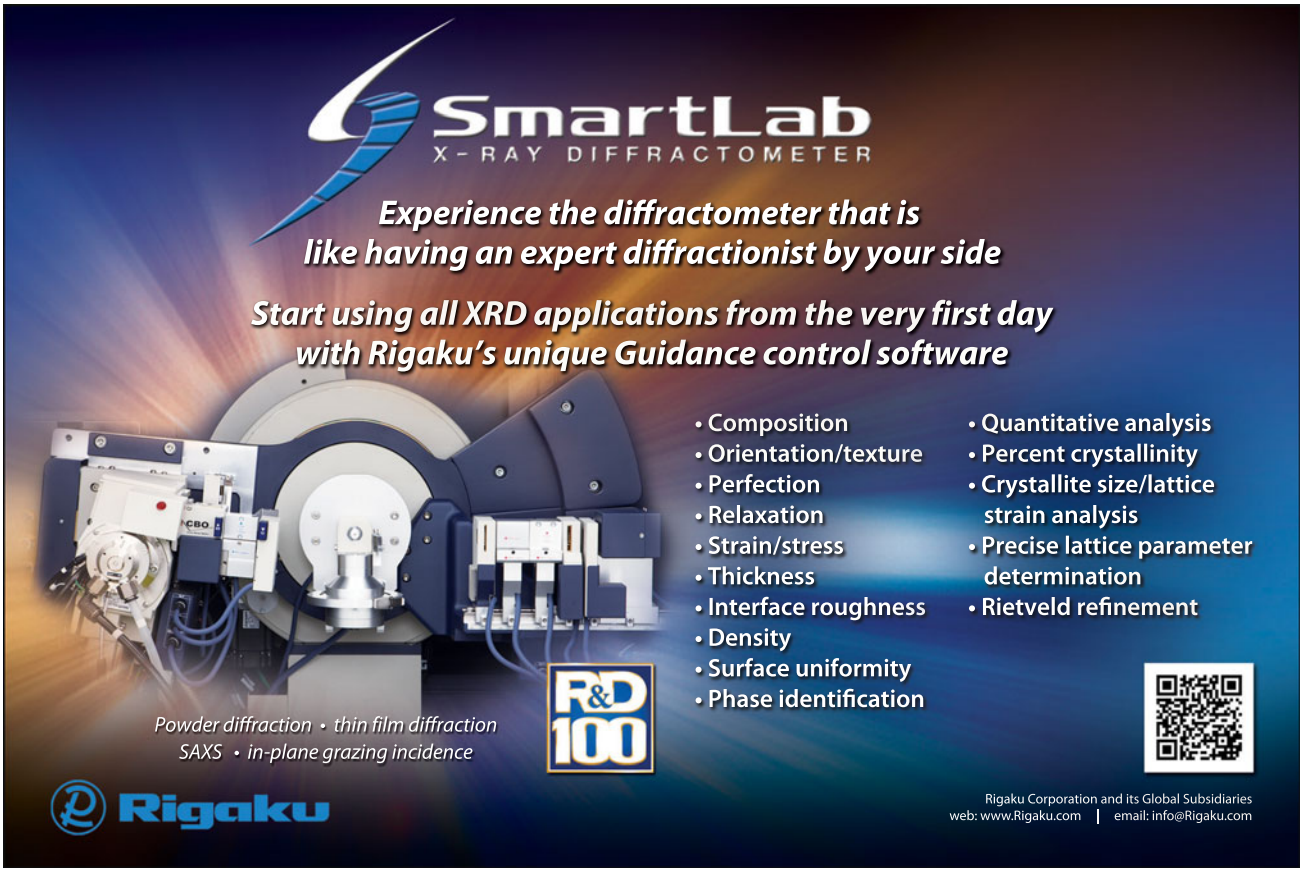
References

1. T.L. Sun, L. Feng, X.F. Gao, L. Jiang, *Acc. Chem. Res.* **38**, 644 (2005).
2. J. Genzer, K. Efimenko, *Biofouling* **22**, 339 (2006).
3. B.X. Leng, Z.Z. Shao, G. de With, W.H. Ming, *Langmuir* **25**, 2456 (2009).
4. C. Lee, C.-J. Kim, *Phys. Rev. Lett.* **106** (2011).
5. X. Zhang, J. Zhao, Q. Zhu, N. Chen, M. Zhang, Q. Pan, *ACS Appl. Mater. Interfaces* **3**, 2630 (2011).
6. H. Jin, M. Kettunen, A. Laiho, H. Pynnonen, J. Paltakari, A. Marmur, O. Ikkala, R.H.A. Ras, *Langmuir* **27**, 1930 (2011).
7. M. Nosonovsky, B. Bhushan, *Curr. Opin. Colloid Interface Sci.* **14**, 270 (2009).
8. X. Huang, X. Wen, J. Cheng, Z. Yang, *Appl. Surf. Sci.* **258**, 8739 (2012).
9. R. Dufour, M. Harnois, Y. Coffinier, V. Thomy, R. Boukherroub, V. Senez, *Langmuir* **26**, 17242 (2010).
10. Z.-G. Guo, W.-M. Liu, *Appl. Phys. Lett.* **90** (2007).
11. M.H. Jin, X.J. Feng, L. Feng, T.L. Sun, J. Zhai, T.J. Li, L. Jiang, *Adv. Mater.* **17**, 1977 (2005).
12. J. Xi, L. Jiang, *Ind. Eng. Chem. Res.* **47**, 6354 (2008).
13. B. Balu, V. Breedveld, D.W. Hess, *Langmuir* **24**, 4785 (2008).
14. Y. Lai, C. Lin, J. Huang, H. Zhuang, L. Sun, T. Nguyen, *Langmuir* **24**, 3867 (2008).
15. P. Kim, T.-S. Wong, J. Alvarenga, M.J. Kreder, W.E. Adorno-Martinez, J. Aizenberg, *ACS Nano* **6**, 6569 (2012).
16. A. Lafuma, D. Quéré, *Europhys. Lett.* **96** (2011).

https://doi.org/10.1557/mrs.2013.101 Published online by Cambridge University Press

17. T.-S. Wong, S.H. Kang, S.K.Y. Tang, E.J. Smythe, B.D. Hatton, A. Grinthal, J. Aizenberg, *Nature* **477**, 443 (2011).
18. D. Richard, D. Quéré, *Europhys. Lett.* **50**, 769 (2000).
19. A. Tuteja, W. Choi, J.M. Mabry, G.H. McKinley, R.E. Cohen, *Proc. Natl. Acad. Sci. U.S.A.* **105**, 18200 (2008).
20. A. Tuteja, W. Choi, M. Ma, J.M. Mabry, S.A. Mazzella, G.C. Rutledge, G.H. McKinley, R.E. Cohen, *Science* **318**, 1618 (2007).
21. A. Tuteja, W. Choi, G.H. McKinley, R.E. Cohen, M.F. Rubner, *MRS Bull.* **33**, 752 (2008).
22. S.S. Chhatre, W. Choi, A. Tuteja, K.C. Park, J.M. Mabry, G.H. McKinley, R.E. Cohen, *Langmuir* **26**, 4027 (2010).
23. A.K. Kota, G. Kwon, W. Choi, J.M. Mabry, A. Tuteja, *Nat. Commun.* **3**, 1025 (2012).
24. J. Yang, Z. Zhang, X. Xu, X. Zhu, X. Men, X. Zhou, *J. Mater. Chem.* **22**, 2834 (2012).
25. S.P.R. Kobaku, A.K. Kota, D.H. Lee, J.M. Mabry, A. Tuteja, *Angew. Chem. Int. Ed.* **51**, 10109 (2012).
26. K. Tsujii, T. Yamamoto, T. Onda, S. Shibuichi, *Angew. Chem. Int. Ed.* **36**, 1011 (1997).
27. T. Young, *Philos. Trans. R. Soc. London* **95**, 65 (1805).
28. R.E. Johnson, R.H. Dettre, in *Contact Angle, Wettability and Adhesion, ACS Advances in Chemistry Series* (American Chemical Society, Washington, DC, 1964), vol. 43.
29. R. Shuttleworth, G.L.J. Bailey, *Discuss. Faraday Soc.* **3**, 16 (1948).
30. A. Marmur, *Langmuir* **19**, 8343 (2003).
31. M. Nosonovsky, *Langmuir* **23**, 3157 (2007).
32. N.A. Patankar, *Langmuir* **19**, 1249 (2003).
33. R.N. Wenzel, *Ind. Eng. Chem.* **28**, 988 (1936).
34. A.B.D. Cassie, S. Baxter, *Trans. Faraday Soc.* **40**, 0546 (1944).
35. W. Chen, A.Y. Fadeev, M.C. Hsieh, D. Oner, J. Youngblood, T.J. McCarthy, *Langmuir* **15**, 3395 (1999).
36. W. Choi, A. Tuteja, J.M. Mabry, R.E. Cohen, G.H. McKinley, *J. Colloid Interface Sci.* **339**, 208 (2009).
37. A. Marmur, *Langmuir* **24**, 7573 (2008).
38. A. Lafuma, D. Quéré, *Nat. Mater.* **2**, 457 (2003).
39. M. Callies, D. Quéré, *Soft Matter* **1**, 55 (2005).
40. S. Herminghaus, *Europhys. Lett.* **79** (2007).
41. W. Choi, A. Tuteja, S. Chhatre, J.M. Mabry, R.E. Cohen, G.H. McKinley, *Adv. Mater.* **21**, 2190 (2009).
42. B. Bhushan, Y.C. Jung, in *Nanotribology and Nanomechanics: Nanotribology, Biomimetics and Industrial Applications* (Springer-Verlag, Berlin, 2011), vol. 2.
43. L.C. Gao, T.J. McCarthy, *Langmuir* **22**, 2966 (2006).
44. Y. Su, B. Ji, Y. Huang, K.-C. Hwang, *Langmuir* **26**, 18926 (2010).
45. A.K. Kota, Y. Li, J.M. Mabry, A. Tuteja, *Adv. Mater.* **24**, 5838 (2012).
46. S. Pan, A.K. Kota, J.M. Mabry, A. Tuteja, *J. Am. Chem. Soc.* **135** (2), 578 (2012).
47. R.E. Johnson, R.H. Dettre, *J. Phys. Chem.* **68**, 1744 (1964).
48. Y. Su, B. Ji, K. Zhang, H. Gao, Y. Huang, K. Hwang, *Langmuir* **26**, 4984 (2010).
49. E. Bittoun, A. Marmur, *Langmuir* **28** (39), 13933 (2012).
50. L. Cao, T.P. Price, M. Weiss, D. Gao, *Langmuir* **24**, 1640 (2008).
51. C.T. Hsieh, F.L. Wu, W.Y. Chen, *J. Phys. Chem. C* **113**, 13683 (2009).
52. D. Wang, X. Wang, X. Liu, F. Zhou, *J. Phys. Chem. C* **114**, 9938 (2010).
53. T. Fujii, Y. Aoki, H. Habazaki, *Langmuir* **27**, 11752 (2011).
54. T. Darmanin, F. Guittard, S. Amigoni, E.T. de Givenchy, X. Noblin, R. Kofman, F. Celestini, *Soft Matter* **7**, 1053 (2011).
55. J. Yang, Z. Zhang, X. Xu, X. Men, X. Zhu, X. Zhou, *New J. Chem.* **35**, 2422 (2011).
56. J.P. Youngblood, N.R. Sottos, C. Extrand, *MRS Bull.* **33**, 732 (2008).
57. J.P. Zhang, S. Seeger, *Angew. Chem. Int. Ed.* **50**, 6652 (2011).
58. H. Wang, Y. Xue, J. Ding, L. Feng, X. Wang, T. Lin, *Angew. Chem. Int. Ed.* **50**, 11433 (2011).
59. D. Bartolo, A. Boudaoud, G. Narcy, D. Bonn, *Phys. Rev. Lett.* **99** (2007).
60. V. Bertola, *Int. J. Heat Mass Transf.* **52**, 1786 (2009).
61. X. Deng, L. Mammen, H.-J.R. Butt, D. Vollmer, *Science* **335**, 67 (2012).
62. X. Wang, X. Liu, F. Zhou, W. Liu, *Chem. Commun.* **47**, 2324 (2011). □

www.mrs.org



https://doi.org/10.1557/mrs.2013.101 Published online by Cambridge University Press